

- ³⁷J. Ducuing, C. Joffrin, and J. P. Coffinet, *Opt. Commun.* **2**, 245 (1970).
- ³⁸F. De Martini, J. Ducuing, and G. Hauchecorne, *IEEE J. Quantum Electron.* **QE-4**, 67 (1968).
- ³⁹S. R. Hartmann, *IEEE J. Quantum Electron.* **QE-4**, 802 (1968).
- ⁴⁰N. Bloembergen and P. S. Pershan, *Phys. Rev.* **128**, 606 (1962).
- ⁴¹M. Born and E. Wolf, *Principles of Optics* (Pergamon, New York, 1964), p. 14.
- ⁴²Equations similar to our Eq. (23) may be found in Ref. 22. However, the equation for $\vec{E}_q(\omega_3)$ reported in Ref. 22 lacks the driving term proportional to $\vec{Q}(\omega_3)$.
- ⁴³An expression similar to our Eq. (26) is reported in Ref. 40 with a misprint: The factor depending on p in Eq. (2.5) of Ref. 40 is written as $\vec{p} - \vec{k}_3(\vec{k}_3 \cdot \vec{p}/k_3^2)$.
- ⁴⁴A. S. Barker, *Phys. Rev.* **165**, 917 (1968).
- ⁴⁵See the work of M. Haas, in *Semiconductors and Semimetals*, edited by R. K. Willardson and A. C. Beer (Academic, New York, 1967), Vol. 3.
- ⁴⁶F. De Martini (unpublished).
- ⁴⁷J. A. Giordmaine, *Phys. Rev. Letters* **8**, 19 (1962).
- ⁴⁸P. D. Maker, R. W. Terhune, M. Nisenhoff, and C. M. Savage, *Phys. Rev. Letters* **8**, 21 (1962).
- ⁴⁹D. A. Kleinman and W. G. Spitzer, *Phys. Rev.* **118**, 110 (1960).
- ⁵⁰D. F. Nelson and E. H. Turner, *J. Appl. Phys.* **39**, 3337 (1968).
- ⁵¹W. Bond, *J. Appl. Phys.* **36**, 1674 (1965).
- ⁵²H. Welcher, *J. Electron.* **1**, 181 (1955).
- ⁵³F. De Martini, C. H. Townes, R. Gustafson, and P. Kelley, *Phys. Rev.* **164**, 312 (1967).
- ⁵⁴J. Cooper, *Nature* **194**, 269 (1962).
- ⁵⁵A. Hadni, *J. Phys. (Paris)* **24**, 694 (1963); A. Hadni, Y. Hanninger, R. Thomas, P. Vergnat, and B. Wyncke, *ibid.* **26**, 345 (1965); A. Hadni, R. Thomas, and J. Perrin, *J. Appl. Phys.* **40**, 2740 (1969).
- ⁵⁶F. Jona and G. Shirane, *Ferroelectric Crystals* (MacMillan, New York, 1962).
- ⁵⁷A fast pyroelectric detector using $\text{Sr}_{1-x}\text{Ba}_x\text{Nb}_2\text{O}_6$ crystals has been reported by A. M. Glass, *Appl. Phys. Letters* **13**, 147 (1968).
- ⁵⁸See the work of E. H. Putley, in *Semiconductors and Semimetals*, edited by R. K. Willardson and A. C. Beer (Academic, New York, 1970), Vol. 5.
- ⁵⁹The stimulated Raman shifts we assumed for the interpretation of the results of our experiments were those reported by G. Eckhardt *et al.*, *Phys. Rev. Letters* **9**, 455 (1962). These data are in good agreement with the values of the spontaneous Raman shifts reported in G. Herzberg, *Infrared and Raman Spectra of Polyatomic Molecules* (Van Nostrand, New York, 1945).
- ⁶⁰I. P. Kaminow and E. H. Turner, *Appl. Opt.* **5**, 1612 (1966).
- ⁶¹In view of the results of the multiple-oscillator theory that describes the linear dynamical behavior of the lattice in GaP, and that involves a frequency-dependent damping parameter $\Gamma(\omega)$ (see Ref. 44), we can assume that the single-oscillator model in the nonlinear regime is only a first approximation picture of the real behavior of the crystal.
- ⁶²R. V. Churchill, *Modern Operational Mathematics in Engineering* (McGraw-Hill, New York, 1965).

Determination of Absolute Signs of Microwave Nonlinear Susceptibilities

M. A. Pollack and E. H. Turner
Bell Telephone Laboratories, Holmdel, New Jersey 07733
 (Received 28 June 1971)

The sign of the microwave nonlinear susceptibility has been found for the first time for a number of acentric crystals. The method used determines the absolute sign without recourse to a comparison crystal. Using known signs of piezoelectric coefficients to specify crystal orientation, all of the nonlinear susceptibilities measured are negative. Predictions of signs and magnitudes of some coefficients in pyroelectric crystals are also made.

INTRODUCTION

Complete specification of a nonlinear susceptibility requires not only that its magnitude be known but also that an algebraic sign related to a defined positive direction in the crystal be given. We describe here a method of finding the absolute signs of microwave nonlinear susceptibility coefficients (d^m) and relate these to positive axes found by piezoelectric tests. We also present the sign results for some crystals in order to complement the recent¹ measurements of the d^m magnitudes. These results, together with recent determinations of the signs of electro-optic¹⁻³ (d^{∞}) and nonlinear optical^{3,4} (d^o)

susceptibilities allow further characterization of materials in terms of Garrett's four-parameter anharmonic-oscillator model.^{1,5} Additionally, in pyroelectric crystals, predictions can be made of magnitudes and signs of some tensor components of d^m other than those directly measured.

The determination⁴ of d^o signs involves comparison with a known crystal. This, in turn, requires that the sign of d^{∞} for at least one crystal be determined⁶ and that its behavior be followed as the modulation frequency is increased through the lattice resonance region.⁷ The d^{∞} sign determination² is also a comparison using a crystal of known⁶ sign. In our method of finding d^m signs, however, each

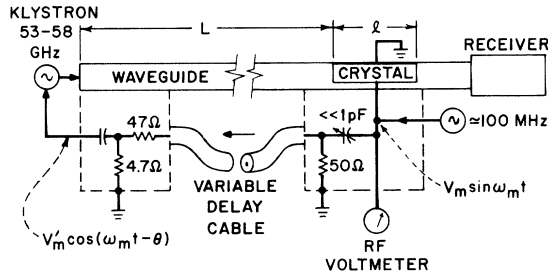


FIG. 1. Experimental arrangement for determining the absolute signs of microwave nonlinear susceptibilities.

measurement is an absolute one in itself.

EXPERIMENTAL METHOD

Both the magnitude and sign of d^m can be measured by generating sidebands, with a low-frequency (~ 100 MHz) modulating field, on a millimeter wave carrier (53–58 GHz) propagating in the crystal under test. The sidebands can be thought of as arising from sum and difference mixing of the carrier and modulating fields through the nonlinear susceptibility d^m . Equivalently, they are associated with phase modulation of the carrier, which results from a variation of the dielectric constant of the crystal induced through d^m by the modulating field. The magnitude of d^m can be determined from the sideband amplitudes.¹ Determination of the sign of d^m requires a comparison of the sideband phases with the phase of the modulating field. In our experiment, the phases of the sidebands produced in the crystal are measured by comparing them with equivalent frequency-modulation sidebands which are generated at the klystron carrier source by modulating its reflector voltage.

The apparatus used is similar to that described elsewhere.^{1,6} It is shown schematically in Fig. 1, where the modifications necessary to this experiment are emphasized. The crystal is oriented so that a positive direction, found, for example, by piezoelectric tests, points toward the ground electrode. As shown in Fig. 1, a small portion of the modulating voltage $V_m \sin \omega_m t$ applied to the crystal under test is used, after amplitude and phase adjustment, to modulate the reflector of the klystron. These adjustments are made to enable the sidebands produced at the klystron to cancel the sidebands produced in the crystal through d^m . It is experimentally convenient to adjust the amplitude of the sampled voltage by means of a voltage divider consisting of a very small variable capacitor ($\ll 1$ pF) and a 50- Ω cable-terminating resistor. This divider also introduces a phase lead of $\frac{1}{2}\pi$, so that the resulting voltage $V'_m \cos \omega_m t$ drives the matched variable-length coaxial line leading to the klystron. The phases of the sidebands produced at the kly-

stron are adjusted by varying the line length, making it imperative that the line be matched so that impedances seen at each end are constant. At the klystron end the coupling network has been designed to introduce virtually no phase shift.

After a variable delay θ , introduced by the line, the modulating voltage applied to the reflector is $V'_m \cos(\omega_m t - \theta)$. The instantaneous klystron frequency is then given by $\omega_t = \omega_0 - c_k V'_m \cos(\omega_m t - \theta)$, where the electrical tuning parameter c_k is always positive. If care is taken to operate the klystron at the center of one of the reflector modes, it can be shown⁹ that no added phase shifts are introduced.

The frequency-modulated output of the klystron then can be described by

$$(\pm 1)^n A J_n(\beta) e^{j[(\omega_0 \mp n\omega_m)t \pm \theta]},$$

where the modulation index $\beta \equiv c_k V'_m / \omega_m$ is the argument of the Bessel's functions J_n and A is an amplitude. The phases of the modulation products are now completely specified because β is always positive. In the experiment we consider only the cancellation of the first sidebands at $\omega_0 \pm \omega_m$ with similar sidebands produced at the nonlinear crystal. Since this sideband amplitude is small, the modulation index β is much less than unity and we can neglect terms in β^2 and higher powers and use $J_0(\beta) = 1$ and $J_1(\beta) = \frac{1}{2}\beta$. The carrier (C), upper sideband (USB), and lower sideband (LSB) fields incident on the crystal can then be written as

$$\begin{aligned} \text{C: } A_i^0 &= A e^{j(\omega_0 t - k_g L)}, \\ \text{USB: } A_i^+ &= -\frac{1}{2} A \beta e^{j[(\omega_0 + \omega_m)t - \theta - \gamma - k_g L]}, \\ \text{LSB: } A_i^- &= +\frac{1}{2} A \beta e^{j[(\omega_0 - \omega_m)t + \theta + \gamma - k_g L]}. \end{aligned} \quad (1)$$

In (1), $k_g L$ is the phase length of the ω_0 wave component, which has a propagation constant k_g in the waveguide of length L between klystron and crystal. The phase lengths in the waveguide structure of the USB and LSB components are $(k_g L + \gamma)$ and $(k_g L - \gamma)$, respectively, where $\gamma \equiv k_0 k_m L / k_g$. The quantities k_0 and k_m are, respectively, free-space propagation constants of the ω_0 and ω_m waves. Over the range of carrier frequencies used, k_0 / k_g is nearly constant, so that γ is only a function of ω_m .

At the nonlinear crystal, the modulating voltage V_m produces a change in the microwave dielectric constant ϵ , given by

$$\Delta\epsilon = 4 d_{eff}^m (V_m / b), \quad (2)$$

where b is the crystal height and d_{eff}^m is the element or combination of elements d_{ijk}^m appropriate to the point group of the crystal and the geometry used. The change in dielectric constant in turn causes a change η in phase length:

$$\eta = -2 d_{eff}^m (V_m / b) (k_0^2 / k_{gc}). \quad (3)$$

In (3), k_{gc} , the propagation constant in the crystal-

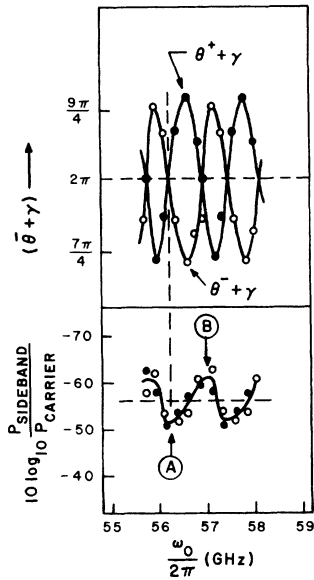


FIG. 2. Measured sideband-to-carrier power ratio and phase delay $(\bar{\theta} + \gamma)$ as functions of carrier frequency ω_0 . Points for the upper sideband are represented by solid circles; those for the lower sideband by open circles. Points A and B occur at maximum and minimum transmission, respectively. Data are for the d_{33}^m coefficient of LiNbO₃: $l = 1.5$ cm, $b = 0.185$ cm, $V_m = 150$ V_{rms}, $\omega_m/2\pi = 81.5$ MHz.

loaded guide, can usually be taken as $\sqrt{\epsilon} k_0$. The time-varying phase length then modulates the wave incident on the crystal. For clarity we consider first an *idealized* case in which the crystal is assumed lossless and matched to the guide. In this case, pure phase modulation is produced and η is the modulation index. The wave components transmitted through the crystal of length l are

$$\begin{aligned} \text{C: } & A_c^o = A' e^{j\omega_0 t}, \\ \text{USB: } & A_+^o = \frac{1}{2} A' e^{j(\omega_0 + \omega_m)t} (\eta - \beta e^{-j(\bar{\theta} + \gamma)}), \\ \text{LSB: } & A_-^o = -\frac{1}{2} A' e^{j(\omega_0 - \omega_m)t} (\eta - \beta e^{j(\bar{\theta} + \gamma)}), \end{aligned} \quad (4)$$

where

$$A' = A e^{-j(k_g L + k_{gc} l)}.$$

In deriving Eq. (4) all terms of second order or higher in η and β have been dropped and we have taken $J_0(\eta) = 1$ and $J_1(\eta) = \frac{1}{2}\eta$. As noted earlier, the crystal is oriented with a positive direction pointing toward the ground electrode; reversal of the crystal changes the sign of η in (4).

In order to obtain cancellation of the $(\omega_0 \pm \omega_m)$ wave components the magnitudes of β and η must be the same, as shown by (4). Recalling that β is always positive, we see that, if η is also positive, cancellation occurs when θ is experimentally adjusted so that $\bar{\theta} + \gamma = 2N\pi$, where N is an integer and $\bar{\theta}$ is the resultant experimental value of θ . On the

other hand, if η is negative the null condition requires $\bar{\theta} + \gamma = (2N + 1)\pi$.

EXPERIMENTAL RESULTS

In the actual experiment the crystals had essentially the same cross section as the waveguide and, because of their high dielectric constants and generally non-negligible losses, were far from being matched. In such a case, the crystal acts as a dielectric resonator in the waveguide, and its transmission shows maxima at $k_{gc}l = n\pi$ and minima at $k_{gc}l = (n + 1/2)\pi$. The measured ratio of sideband-to-carrier power, shown in Fig. 2 as a function of carrier frequency ω_0 for a typical crystal (LiNbO₃), also exhibits resonant behavior. The sideband components now contain contributions from amplitude as well as phase modulation. In spite of this added complexity, $|\eta|$ can be obtained directly, as analysis indicates that $10 \log_{10}(|\eta|^2/4)$ equals the average of the logarithmic sideband-to-carrier ratios at the transmission maxima (point A) and minima (point B). The magnitude of d^m can then be obtained by using (3).

The phase condition on $(\bar{\theta} + \gamma)$ for cancellation of the sideband components is also a function of carrier frequency in the resonant case (Fig. 2). In general, the phase delay required for cancellation of the upper- and lower-sideband components are different, and we denote them by θ^+ and θ^- , respectively. However, at points A and B, $\theta^+ = \theta^- = \bar{\theta}$, and the cancellation condition reverts to the simple one in the ideal case above: $(\bar{\theta} + \gamma) = 2N\pi$ if $\eta > 0$. If one departs, for example, from the $k_{gc}l = n\pi$ condition (point A) by increasing ω_0 , cancellation requires an increase in θ^+ and a decrease in θ^- (Fig. 2). The changes in θ^+ and θ^- result both from phase-modulation shifts and from amplitude-modulation products. The difference between θ^+ and θ^- is not small: We compute in a typical case that $\theta^+ - \theta^- = \frac{1}{2}\pi$ for $k_{gc}l = (2n + 1)\frac{1}{4}\pi$ if $R e^{-2\alpha l} = 0.5$, where R is the power-reflection coefficient at one crystal face and 2α is the power-attenuation coefficient. Our analysis shows, however, that for arbitrary $k_{gc}l$ the null condition requires $\frac{1}{2}(\theta^+ + \theta^-) + \gamma = 2N\pi$ for $\eta > 0$. Our measurements were made on both sidebands at a number of values of ω_0 , thereby varying k_{gc} . The experiment and analysis agree with regard to requirements on θ^+ and θ^- as well as on amplitude cancellation requirements.

We have used piezoelectric tests in order to establish a direction to which the signs of the d^m could be related. Similar tests have been used in d^{90} (Ref. 2) and d^o (Ref. 4) sign determinations and have been related¹⁰ to pyroelectric effect and spontaneous polarization in polar crystals as well as to atomic ordering. In all cases we have used the "parallel" geometry¹ in which modulating field and microwave field are parallel. Since the piezoelec-

TABLE I. Signs of piezoelectric and measured nonlinear microwave susceptibility coefficients.

Material	Point group	Tensor component ^a d_{ijk}	Piezoelectric sign	d_{ijk}^m sign
BaTiO ₃	4mm	d_{333}	+	-
LiTaO ₃	3m	d_{333}	+	-
LiNbO ₃	3m	d_{333}	+	-
LiIO ₃	6	d_{333}	+	-
KH ₂ PO ₄	$\bar{4}2m$	$\frac{1}{3}(2d_{231} + d_{123})$	+	-
NH ₄ H ₂ PO ₄	$\bar{4}2m$	$\frac{2}{3}(2d_{231} + d_{123})$	+	-
ZnO	6mm	d_{333}	+	-
CdS	6mm	d_{333}	+	-
GaP	$\bar{4}3m$	d_{123}	-	-
GaAs	$\bar{4}3m$	d_{123}	-	-

^aApart from a multiplying factor for $\bar{4}2m$ and $\bar{4}3m$ crystals, these components are appropriate for longitudinal-piezoelectric and parallel-nonlinear coefficients.

tric tensors and d^m tensors have the same form, it is not surprising that this geometry is also one in which a "longitudinal" piezoelectric effect¹¹ exists: A compressional stress applied parallel to the field directions in the d^m experiments produces a change in polarization in the same direction. A positive [111] direction in the $\bar{4}3m$ crystals or the positive [001] in the 6mm crystals are defined as the direction from cation to the nearest-neighbor anion lying in the appropriate direction. In Table I we list the piezoelectric signs used in identifying these axes. The positive c -axis direction in the pyroelectric crystals coincides with the sense of the spontaneous polarization. In the $\bar{4}2m$ crystals both piezoelectric coefficients are taken as positive¹² and this allows one to find a positive axis.

Using positive axes described above, we find that all of the d_{ijk}^m we have measured are negative (see Table I).

DISCUSSION

In the II-VI and III-V compounds, the microwave nonlinearity appears to be closely related to atomic ordering, which determines the axis sense. The negative sign of the combination ($2d_{231}^m + d_{123}^m$) found for the $\bar{4}2m$ crystals probably¹³ means that each of

the coefficients is negative, as one would expect from the Kleinman condition¹⁴ allowing complete permutation of indices.

In LiNbO₃, it is possible to predict the observed sign of d_{333}^m from the variation of dielectric constant with temperature. The constant-strain dielectric constants ϵ_3^s and ϵ_1^s both increase with increasing temperature.¹⁵ If we assume that the entire change in ϵ_i^s can be related to a change in spontaneous polarization ΔP_s , acting through d_{i13} , we can write

$$\frac{\Delta\epsilon_i^s}{\Delta T} = \frac{4d_{i13}^m}{\epsilon_o(\epsilon_i^s - 1)} \frac{\Delta P_s}{\Delta T}, \quad (5)$$

where ΔT is a temperature increment. Since $(\Delta P_s/\Delta T) < 0$ and $(\Delta\epsilon_i^s/\Delta T) > 0$, then $d_{i13}^m < 0$. Thus, in addition to correctly predicting the observed negative sign of d_{333}^m , we also anticipate that d_{113}^m is negative. In using Eq. (4) one should note that constant-stress values of d_{i13}^m are actually more appropriate than the constant-strain value found in the microwave experiments. Also, differences between low- and high-frequency dielectric constants, volume changes, and temperature dependence of d_{i13}^m are neglected. Assuming that these factors affect $\Delta\epsilon_1^s$ and $\Delta\epsilon_3^s$ in a similar fashion, however, the ratio

$$\frac{(\Delta\epsilon_1^s/\Delta T)}{(\Delta\epsilon_3^s/\Delta T)} = \frac{d_{113}^m(\epsilon_3^s - 1)}{d_{333}^m(\epsilon_1^s - 1)} \quad (6)$$

can be used with the experimental values of $\Delta\epsilon_i^s$ to predict that $d_{113}^m \approx d_{333}^m$. Uncertainties in the value of ΔP_s are also eliminated by using (6).

Jerphagnon¹⁶ has developed a relationship between the spontaneous polarization P_s and the vector parts of the optical and electro-optical nonlinear coefficients for pyroelectric crystals. It is possible to adapt this notion to the microwave nonlinearities, so that we can use the magnitudes¹ and newly measured signs of d_{333}^m to predict magnitudes and signs of d_{113}^m . Following Jerphagnon and defining¹⁷ $\delta_{333}^m \equiv d_{333}^m/(\epsilon_3^s - 1)^3$ and $\delta_{113}^m \equiv d_{113}^m/(\epsilon_1^s - 1)^2(\epsilon_3^s - 1)$, we can write, in the δ formulation

$$\delta_{333}^m + 2\delta_{113}^m = K P_s. \quad (7)$$

The constant K can be evaluated from the data

TABLE II. Values of constant-strain dielectric constants, spontaneous polarization (in C/m²), microwave nonlinear coefficients (in 10⁻¹² m/V), and δ coefficients (in 10⁻¹² m/V) for pyroelectric materials. Values of ϵ_1^s and ϵ_3^s are taken from current literature. The value of P_s for LiIO₃ has been estimated in Ref. 16, and the other values are tabulated there. Magnitudes of d_{333}^m are from Ref. 1.

Material	ϵ_1^s	ϵ_3^s	P_s	d_{333}^m	δ_{333}^m	δ_{113}^m	d_{113}^m
LiNbO ₃	43	25.5	0.71	-6700	-0.46	-0.16	-6700
LiTaO ₃	41	40	0.50	-16 000	-0.27	-0.14	-8700
BaTiO ₃	2300	57	0.26	-97 000	-0.55	+0.13	+3.9(10 ⁷)
LiIO ₃	8	6.53	1.45	-177	-1.05	-0.27	-74

for LiNbO_3 given in Table II, along with the above estimate that $d_{113}^m \approx d_{333}^m$ for this material. We find that $K = -1.1(10^{-12}) \text{ m}^3/\text{J}$. Predicted values of δ_{113}^m and d_{113}^m are given in Table II for some other pyroelectric crystals for which d_{333}^m is known. The positive sign and enormous magnitude anticipated for d_{113}^m in BaTiO_3 are most interesting. All of

these predictions await experimental verification.

ACKNOWLEDGMENTS

It is a pleasure to acknowledge the encouragement of G. D. Boyd in the course of this work and the helpful comments of G. A. Coquin on the manuscript.

¹G. D. Boyd, T. J. Bridges, M. A. Pollack, and E. H. Turner, *Phys. Rev. Letters* **26**, 387 (1971). In Eq. (2) of this reference d_{eff}^2 should be d_{eff}^2 .

²E. H. Turner (unpublished).

³R. C. Miller, S. C. Abrahams, R. L. Barns, J. L. Bernstein, W. A. Nordland, and E. H. Turner, *Solid State Commun.* **9**, 1463 (1971).

⁴R. C. Miller and W. A. Nordland, *Opt. Commun.* **1**, 400 (1970); R. C. Miller and W. A. Nordland, *Phys. Rev. B* **2**, 4896 (1970).

⁵C. G. B. Garrett, *J. Quantum Electron.* **4**, 70 (1968).

⁶D. F. Nelson and E. H. Turner, *J. Appl. Phys.* **39**, 3337 (1968).

⁷W. L. Faust and C. H. Henry, *Phys. Rev. Letters* **17**, 1265 (1966).

⁸T. J. Bridges, G. D. Boyd, and M. A. Pollack, *Proceedings of the Symposium on Submillimeter Waves*, Vol. 20 of *Microwave Research Institute Symposia Series* (Polytechnic, Brooklyn, New York, 1971).

⁹D. R. Hamilton, J. K. Knipp, and J. H. B. Kuper,

Klystrons and Microwave Triodes (McGraw-Hill, New York, 1948).

¹⁰A more complete discussion of the orienting problem and a number of references can be found in Ref. 4.

¹¹J. F. Nye, *Physical Properties of Crystals* (Clarendon, Oxford, England, 1957), p. 127.

¹²*Proc. IRE* **37**, 1387 (1949).

¹³In Ref. 1 experiment showed $\frac{1}{3}|2d_{231}^m + d_{123}^m| \approx |d_{123}^m|$, and it was deduced that $d_{121}^m = d_{123}^m$.

¹⁴D. A. Kleinman, *Phys. Rev.* **126**, 1977 (1962).

¹⁵K. Nassau, H. J. Levinstein, and G. H. Loiacono, *J. Phys. Chem. Solids* **27**, 989 (1966).

¹⁶J. Jerphagnon, *Phys. Rev. B* **2**, 1091 (1970).

¹⁷It is not clear whether the δ_{AB} of Ref. 1 would have been more appropriate here. However, the difference in the δ 's is less than the sort of error expected in this calculation.

¹⁸S. H. Wemple, M. DiDomenico, Jr., and I. Camlibel, *Appl. Phys. Letters* **12**, 209 (1968).

Dielectric Properties of Lithium Hydrizinium Sulfate[†]

V. Hugo Schmidt* and John E. Drumheller

Department of Physics, Montana State University, Bozeman, Montana 59715

and

Francis L. Howell

Department of Physics, University of North Dakota, Grand Forks, North Dakota 58201

(Received 30 April 1971)

The dc conductivity and ac dielectric susceptibility of normal and deuterated lithium hydrizinium sulfate have been measured over a wide temperature range at frequencies up to 9.33 GHz. Over a very large temperature and frequency range the real and imaginary parts of the susceptibility are very large (up to $\epsilon' \approx \epsilon'' \approx 10^6$) and vary with frequency somewhat as $f^{-1/2}$. This unusual behavior is shown to result from the nearly one-dimensional protonic conductivity and its extreme sensitivity to barriers caused by local structural defects. Etching studies indicate that the crystal is not ferroelectric, implying that the apparent hysteresis loops result from saturation of the ac conduction.

I. INTRODUCTION

Lithium hydrizinium sulfate ($\text{LiN}_2\text{H}_5\text{SO}_4$) has been generally considered to be a member of the ferroelectric sulfate family¹ because it exhibits what appear to be hysteresis loops, although no conclusive evidence for a ferroelectric phase transition has been found. At the same time, it exhibits unusually large protonic conductivity along the "ferroelectric"

c axis.^{1,2} It has been previously suggested that this crystal is not ferroelectric, and that its anomalous dielectric behavior is caused by protons in the hydrizinium chains which run along the c axis, but no detailed explanation was given.³ We present herein a model which assumes partially blocked current flow along the hydrizinium ion chains and which predicts no hysteresis in the dc limit. Good qualitative agreement with our experimental results is ob-